Chemical Engineering Journal 156 (2010) 613–617

Contents lists available at ScienceDirect

Chemical Engineering Journal

journal homepage: www.elsevier.com/locate/cej

Thermodynamic properties of a new working pair: 1-Ethyl-3-methylimidazolium ethylsulfate and water

Guilan Zuo, Zongchang Zhao*, Shuanghua Yan, Xiaodong Zhang

Research Institute of Chemical Engineering, Dalian University of Technology, 158 Zhong Shan Road, Dalian 116012, PR China

ARTICLE INFO

Article history:
Received 18 October 2008
Received in revised form 21 March 2009
Accepted 4 June 2009

Keywords:
Ionic liquid
Vapor pressure
Density
Heat capacity
NRTL model

ABSTRACT

Vapor pressures, heat capacities and densities of the 1-ethyl-3-methylimidazolium ethyl sulfate (EMISE) + water were measured at the various temperatures and ionic liquid concentrations. The system was chosen as a novel candidate for organic working pairs for an absorption heat pump. The vapor pressures of the solution were correlated by the NRTL model, the heat capacity and density of the solution were correlated by the polynomial equation as a function of temperature and concentration, and the parameters in the regression equation were determined by a Levenberg–Marquardt method, the average relative deviations between the experimental and calculated values in vapor pressure, heat capacity and density measurements were 1.9%, 1.2%, 0.8%, respectively. The vapor pressures of the solution decreases with the decrease in solution temperature and with the increase in EMISE mole concentration, the heat capacity of the solution decreases with EMISE mole concentration at the same temperature and slightly increases with increasing temperature at the same concentration. The density of the solution decreases with increasing temperature and water mole concentration.

© 2009 Elsevier B.V. All rights reserved.

1. Introduction

Absorption heat pump is important for recovering industry waste heat. Until now, the working pairs in the absorption heat pump systems are mainly ammonia–water and lithium bromide–water [1]. However, ammonia–water fluids are known to have disadvantages of high working pressure and toxicity, whereas water–lithium bromide mixture has disadvantages of corrosion and crystallization [2]. Thus, it is absolutely necessary to explore new working pairs that can overcome the serious corrosion and crystallization problems.

Ionic liquids (ILs) are a class of low-temperature molten salts which are constituted by an organic cation and an inorganic anion. In recent years, ILs have been used as organic green solvent in catalysis, separation process, electrochemistry and many other industries because of unique physical and chemical properties, such as negligible vapor pressure, stable in the air and water, a wide liquid range, with melting point below 373 K [3,4], and relatively favorable viscosity and density characteristics. Due to these features, it is possible that ionic liquids could be used as the novel working fluids in the absorption heat pump [5–7].

In this research, the binary solution 1-ethyl-3-methylimidazolium ethylsulfate (EMISE)–water was chosen as a potential working fluid. The ionic liquid EMISE acts as absorbent and water as refrigerant. Water has a good solubility in the EMISE because of the permanent ion–dipole interaction, and EMISE can be easily separated from water by heating the solution because ionic liquid have no detectable vapor pressure. In order to decide whether the EMISE–water system is suitable as a novel working pair for absorption heat pump or not, several thermodynamic properties of the working fluid such as the vapor pressure, heat capacity, and density were measured at different temperatures and IL-concentrations to provide the basic information for the potential use of the EMISE–water system, the vapor–liquid equilibrium (VLE) data were measured by the boiling point method and analyzed with the nonrandom two-liquid (NRTL) model, and the experimental data of heat capacity and density were satisfactorily correlated with the simple polynomial functions of temperature and molar fraction. These basic data are very useful and necessary for calculating the performance of an absorption heat pump.

2. Experimental

2.1. Materials

The 1-methylimidazole was a kind of commercial product with the purity of 99%, diethyl sulfate (≥99%) and toluene (≥99%) were supplied by Tianjin Fuchen Reagents Company, the purity of the

* Corresponding author. Tel.: +86 411 88993626; fax: +86 411 83633080.
E-mail addresses: zuoguilan@hotmail.com (G. Zuo), zczhao55@163.com (Z. Zhao).

1385-8947/$ – see front matter © 2009 Elsevier B.V. All rights reserved.
doi:10.1016/j.cej.2009.06.020

reagents was checked by gas chromatogram (GC2010, Japan). All reagents were further purified by distillation and degassed before used.

2.2. Synthesis of 1-ethyl-3-methylimidazolium ethyl sulfate

1-Ethyl-3-methylimidazolium ethyl sulfate was prepared according to literature procedure [8]. 282.48 g (240 mL, 1.83 mol) of diethyl sulfate was dropped to 123.6 g (120 mL, 0.8 mol) of 1-methylimidazole in toluene (150 mL) and maintain the reaction temperature below 313.15 K due to the reaction being highly exothermic. The reaction mixture was stirred at room temperature for 4 h. The IL product was immediately formed and it is initially clear solution and then opaque, followed by biphasic separation of the toluene solution and formation of a denser IL phase. The upper phase was decanted, and the lower phase was washed with toluene three times, each time with 70 mL toluene. After the last washing, the remaining toluene was removed by rotary evaporation under reduced pressure of 343.15 kPa. The ionic liquid obtained was dried by heating to 353.15 K and under high vacuum (10 kPa) for 10 h. The resulting liquid was a colorless ionic liquid. It was characterized with ^{1}H NMR (400 MHz, D_2O, ppm), ^{1}H spectra of the product showed the same with the literature [9]. The purity was more than 98.9% in terms of liquid chromatography.

2.3. Vapor pressure measurements

The vapor pressures were measured by the boiling point method [10]. This method is valid because the vapor pressure of the ionic liquid is neglectable compared with the vapor pressure of water [11–15]. The apparatus was consisted of an equilibrium flask of 500 cm^3, a constant-temperature bath, a condenser, a U-tube mercury manometer capable of reading to 1 mmHg and a thermometer capable of reading to 0.1 °C, a schematic diagram is shown in Fig. 1. The initial sample solution with a desired absorbent (IL) molar concentration was prepared by weighing a certain amount of IL and water with a counter balance with the uncertainty of ±0.02 g, and then pulled them into the flask and evacuated to a proper pressure. The sample solution was then heated, when the thermal equilibrium was reached, the temperature of the sample solution and the pressure of the apparatus were measured. The initial concentration of each sample solution was calculated and varied by pulling the water into the solution. The final concentration of the each sample solution was rectified by subtracting the amount of the condensate in the condenser.

The vapor pressures of the binary solution EMISE + water were measured in the mole fraction of the EMISE range from 0.545 to 0.109 and the temperature range from 312.20 to 373.35 K. The experimental results were listed in Table 1 and plotted in Fig. 2.

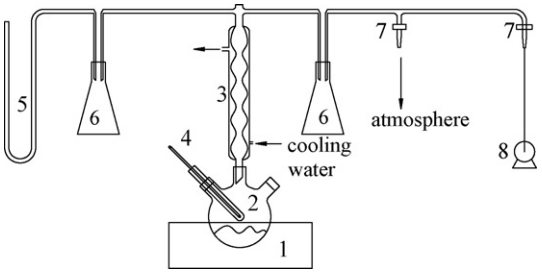

Fig. 1. Experimental apparatus for vapor pressure measurements: (1) electric heating jacket, (2) sample vessel, (3) condenser, (4) thermometer, (5) mercury manometer, (6) buffer flask, (7) needle valve, and (8) vacuum pump.

Table 1
Vapor pressure data and activity coefficients of binary system water (1) + EMISE (2).

T (K)	p^{exp} (kPa)	p^{NRTL} (kPa)	Δ (%)
x_2 = 0.545			
341.15	4.21	4.18	0.7
348.15	6.51	6.27	3.7
354.95	9.33	9.06	2.9
360.15	12.13	11.78	2.9
364.15	14.40	14.25	1.0
368.15	17.39	17.07	1.8
371.15	19.85	19.41	2.2
373.35	22.13	21.29	3.8
x_2 = 0.446			
341.85	5.81	5.97	2.8
347.55	8.29	8.27	0.3
353.25	11.49	11.23	2.3
357.55	14.16	13.98	1.3
360.25	15.68	15.94	1.7
361.95	16.80	17.28	2.9
364.95	19.20	19.84	3.3
368.25	22.35	22.98	2.8
x_2 = 0.341			
335.75	5.63	5.81	3.2
341.65	8.13	8.25	1.5
347.05	11.07	11.16	0.8
351.15	13.63	13.87	1.7
354.65	16.29	16.23	0.4
358.25	19.17	19.77	3.1
361.05	22.08	22.56	2.2
363.15	24.75	24.85	0.4
x_2 = 0.226			
328.45	6.13	6.05	1.3
334.35	8.27	8.09	2.2
339.05	11.15	10.63	4.7
343.75	13.92	13.77	1.1
346.85	16.40	16.21	1.2
349.75	19.33	18.80	2.7
352.65	21.87	21.71	0.7
355.15	24.56	24.49	0.3
x_2 = 0.109			
320.35	6.11	6.03	1.3
326.25	8.75	8.61	0.2
330.95	11.33	11.28	0.4
335.45	14.27	14.37	0.7
338.55	16.75	16.78	0.2
341.45	19.07	19.56	2.6
344.25	21.92	22.45	2.4
346.75	24.67	25.31	2.6
			ARD = 1.9%

$\Delta = \frac{|p^{exp} - p^{cal}|}{p^{exp}}$.

$\text{ARD} = \frac{1}{n}\sum_{i=1}^{n} \frac{|p^{cal} - p^{exp}|}{p^{exp}}$.

2.4. Heat capacity measurements

An isoperibol solution calorimeter was used to measure the heat capacity of the sample solutions. The calorimeter consists of a constant bath, a calibration heater with 100 Ω resistance, a stirring rod and a vessel for containing the sample solution. The sample solutions with desired absorbent (IL) concentration were also prepared by weighing a certain amount of IL and water with a counter balance with the uncertainty of ±0.02 g. All the sample solutions were prepared immediately prior to performing measurement in order to avoid variations of the composition due to the ionic liquid EMISE absorbing the water vapor in the air. The accurately weighted sample solution of the desired concentration was placed into the vessel. The calibration heater and stirring rod were immersed when the vessel was clamped on the main body of the solution calorimeter. The stirrer and heater were turned on to heat up the sample solution to a temperature slightly lower than desired. After being heated

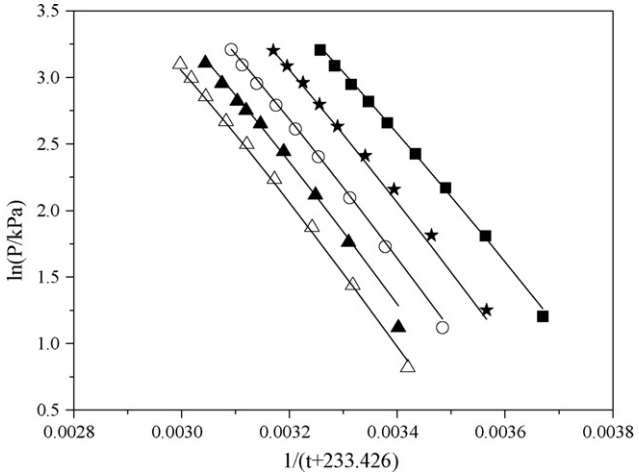

Fig. 2. The vapor pressure of binary solution water (1) + EMISE (2) at different mole fractions of EMISE: —, calculated by NRTL equation; symbols are experimental data at different mole fractions of EMISE: △, 0.545; ▲, 0.446; ○, 0.341; ⋆, 0.226; ■, 0.109.

about 30 s the heater was turned off. The accurate amount of heat added was calculated through measuring the current and voltage values with a digital voltmeter and corresponding time. The uncertainty of the voltage, current and time was 0.01 V, ±0.001 A and 0.01 s, respectively. The temperature difference during the heating process was also measured and was used to calculate the heat capacity of the sample solution with the following equation.

$$Q = (mC_p + \varepsilon)\Delta T \quad (1)$$

$$Q = UIt \quad (2)$$

where Q is the total amount of the heat added, m is the mass of the sample solution, C_p is heat capacity (kJ/kg/K) of the sample, and ε is the heat capacity (kJ/K) of the apparatus including the vessel, stirring rod, heater. The value of the ε was calculated by the experimental result using pure glycerol as a sample solution and its known heat capacity value at each temperature considered. The experimental apparatus was checked first with deionized water listed in Table 2, it showed good agreement with the literature [16] and the average relative deviation was 1.3%. The experimental heat capacity of the pure EMISE at different temperatures were also showed good agreement with the literature [17], which were listed in Table 3 and the average relative deviation was 0.3%. The heat capacity of the binary solution EMISE + H_2O was measured in the whole molar concentration range of the EMISE and the temperature range from 303.15 to 323.15 K. The experimental results were listed in Table 4.

Table 2
Comparison of the heat capacity of pure water C_p^{exp} measured in this work with those C_p^{lit} available from the literature [16].

T (K)	C_p^{exp} (kJ/kg/K)	C_p^{lit} (kJ/kg/K)	Δ (%)
303.15	4.126	4.174	1.2
308.15	4.130	4.174	1.1
313.15	4.110	4.174	1.5
318.15	4.119	4.174	1.3
323.15	4.125	4.174	1.2
			ARD = 1.3%

$\Delta = \frac{|C_p^{exp} - C_p^{lit}|}{C_p^{exp}}$.

$\text{ARD} = \frac{1}{n}\sum_{i=1}^{n} \frac{|C_p^{exp} - C_p^{exp}|}{P^{exp}}$.

Table 3
Comparison of the heat capacity of pure EMISE C_p^{exp} measured in this work with those C_p^{lit} available from the literature [17].

T (K)	C_p^{exp} (kJ/kg/K)	C_p^{lit} (kJ/kg/K)	Δ (%)
303.15	1.608	1.605	0.2
308.15	1.614	1.609	0.3
313.15	1.619	1.614	0.3
318.15	1.624	1.619	0.3
323.15	1.630	1.625	0.3
			ARD = 0.3%

Table 4
Experimental heat capacity for the binary system water (1) + EMISE (2).

x_2	C_p (kJ/kg/K) at the following T (K)				
	303.15	308.15	313.15	318.15	323.15
0.099	2.744	2.767	2.856	2.948	3.072
0.290	2.070	2.103	2.117	2.155	2.208
0.499	1.903	1.924	1.941	1.969	1.999
0.691	1.781	1.838	1.860	1.872	1.901
1	1.608	1.614	1.619	1.624	1.630

Table 5
Comparison of the density of pure water ρ_{exp} measured in this work with those ρ_{lit} available from the literature [16].

T (K)	ρ_{exp} (g/cm^3)	ρ_{lit} (g/cm^3)	Δ (%)
303.15	0.9957	0.9957	0
308.15	0.9929	0.9941	0.2
313.15	0.9910	0.9922	0.1
318.15	0.9881	0.9902	0.1
323.15	0.9871	0.9882	0.2
			ARD = 0.1%

$\Delta = \frac{|\rho_{exp} - \rho_{lit}|}{\rho_{exp}}$.

$\text{ARD} = \frac{1}{n}\sum_{i=1}^{n} \frac{|\rho_{exp} - \rho_{lit}|}{\rho_{exp}}$.

2.5. Density measurements

The solution of water and EMISE were prepared by mass using a counter balance, precise to ±0.02 g. All the samples were prepared immediately prior to performing density measurement to avoid variations in the composition due to the ionic liquid EMISE is easy to absorb the water vapor in the air. The density of the binary solution EMISE + water were accurately measured in whole molar concentration range of the EMISE and the temperature range from 303.15 to 323.15 K at the atmospheric pressure using a specific gravity balance, the uncertainty in the experimental measurements was less than ±0.0001 g/cm^3 and the precision of the temperature was 0.1 °C. The specific gravity balance was calibrated by measuring the density of the deionized water and the results listed in Table 5, which showed good agreement with the literature values [16] within 0.1% average relative error. The experimental results were listed in Table 6.

Table 6
Experimental density for the binary system water (1) + EMISE (2).

x_2	ρ (g/cm^3) at the following T (K)				
	303.15	308.15	313.15	318.15	323.15
0.201	1.2023	1.1989	1.1949	1.1919	1.1888
0.410	1.2392	1.2362	1.2330	1.2295	1.2267
0.581	1.2509	1.2479	1.2453	1.2422	1.2391
0.787	1.2591	1.2541	1.2512	1.2477	1.2448
1	1.2650	1.2617	1.2587	1.2555	1.2523

Table 7
Comparison of the vapor pressure of pure water P^{exp} measured in this work with those P^{lit} available from the literature [18].

T (K)	P^{exp} (kPa)	P^{lit} (kPa)	Δ (%)
351.45	44.29	44.21	0.2
352.65	46.56	46.43	0.3
353.95	49.33	48.93	0.8
355.15	51.94	51.35	1.2
356.25	54.61	53.65	1.8
357.55	57.22	56.47	1.3
358.65	59.54	58.96	1.0
359.75	62.15	61.54	1.0
			ARD = 1.0%

3. The correlation of experimental results and discussion

3.1. Vapor pressure

In order to check the reliability of the experimental apparatus, vapor pressure measurements of pure water have been performed by the boiling point method. Results of our measurements for vapor pressures of pure water are compared in Table 7 with those well-established in the literature [18]. It can be found that the deviations of vapor pressures of deionized water measured in this experimental apparatus from the ones in the literature are within 1.0% average relative deviation, which implies that the experimental apparatus is reliable and applicable for the measurement of vapor pressure for IL-containing systems.

In present research, the experimental vapor pressures of the solution EMISE + water were predicted by the following non-electrolyte NRTL equation [19]. Eq. (3) has been used to determine activity coefficients γ_1 from experimental data of partial pressures P_1 including the vapor pressure of the pure water P_1^0.

$$P_1 = p_1^0 x_1 \gamma_1^{NRTL} \tag{3}$$

For binary system containing ionic liquid, for example, solvent (1) + ionic liquid (2), the vapor phase is fully composed of solvent vapor due to the negligible volatility of IL, the NRTL equation of the binary system can be described as follows.

$$\ln \gamma_1 = x_2^2 \left[\tau_{21} \left(\frac{G_{21}}{x_1 + x_2 G_{21}} \right)^2 + \frac{\tau_{12} G_{12}}{(x_2 + x_1 G_{12})^2} \right] \tag{4}$$

$$\ln\ \gamma_2 = x_1^2 \left[\tau_{12} \left(\frac{G_{12}}{x_2 + x_1 G_{12}} \right)^2 + \frac{\tau_{21} G_{21}}{(x_1 + x_2 G_{21})^2} \right] \tag{5}$$

where

$$G_{12} = \exp(-\alpha \tau_{12}), \quad G_{21} = \exp(-\alpha \tau_{21}) \tag{6}$$

For the equation, the α, τ_{12} and τ_{21} are the binary model parameters. In order to consider the temperature dependency of parameters τ_{12} and τ_{21} in NRTL model, a following formula containing four parameters was adopted for correlation.

$$\tau_{12} = a + \frac{b}{T} \tag{7}$$

$$\tau_{21} = c + \frac{d}{T} \tag{8}$$

The parameters a, b, c, d and α in the NRTL model were obtained by fitting the experimental vapor pressure data in the temperature range from 312.20 to 373.35 K and the composition of the EMISE rang from 0.545 to 0.109 using Levenberg–Marquardt method. They are respectively as shown in Tables 1 and 8 and Fig. 2. The experimental vapor pressures can be well correlated by adopting NRTL model with interaction parameters formula containing four parameters, the average relative deviation (ARD) between the predicted and experimental value was less than 1.9%.

Table 8
NRTL model parameters obtained by correlating activity coefficients of water (1) + EMISE (2).

	τ_{12} (J/mol)		τ_{21} (J/mol)	α
a	−11.2281	c	2.5165	1.0985
b	4439.0252	d	−1439.5482	

The variation of the vapor pressure versus the temperature at different IL-content was shown in Fig. 2 for water + EMISE system. It is seen that the vapor pressure of the solvent decreases with the decrease of solution temperature and lower the vapor pressure of the solvent higher the IL-content is.

The solubility of a refrigerant in an absorbent is one of the major factors for deciding the suitability of a working fluid. It mainly depends on the interaction between the refrigerant and the absorbent and the vapor pressure depreciation. The vapor pressure measurement can be a method to evaluate the affinity between a refrigerant and an absorbent. Fig. 3 shows the vapor pressures depreciation of the solution EMISE + H_2O at 323.15 K. The permanent ion–dipole interaction between the ionic liquid and water evokes a considerable negative deviation from Raoult's law, which is a basic characteristic of absorption working pairs [20].

3.2. Heat capacity

The heat capacity of the binary solution EMISE + H_2O was measured at the temperature range from 303.15 to 323.15 K and molar fraction of the EMISE from 0 to 1. The experimental results are listed in Table 4 and plotted in Fig. 4 and are simply fitted with the following equation [21].

$$C_p = \sum_{i=0}^{3} (a_i + b_i T) x^i \tag{9}$$

where C_p is the heat capacity in kJ/kg/K, a_i and b_i are the regression parameters, T is the absolute temperature in K, and the x is the molar fraction of the EMISE. The regression parameters were determined by a least-squares method and listed in Table 9. The average relative deviation (ARD) was 1.2% between the experimental and calculated values. The heat capacity of the solution decreased with EMISE mole concentration at the same temperature and slightly increased with increasing temperature at the same concentration.

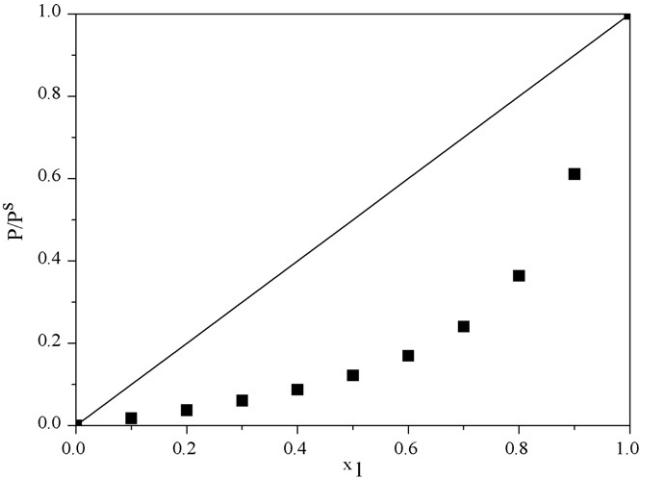

Fig. 3. The prediction of the vapor pressure for the EMISE + H_2O at 323.15 K: ■, real solution; —, ideal solution; P, vapor pressure; P_S, vapor pressure of H_2O.

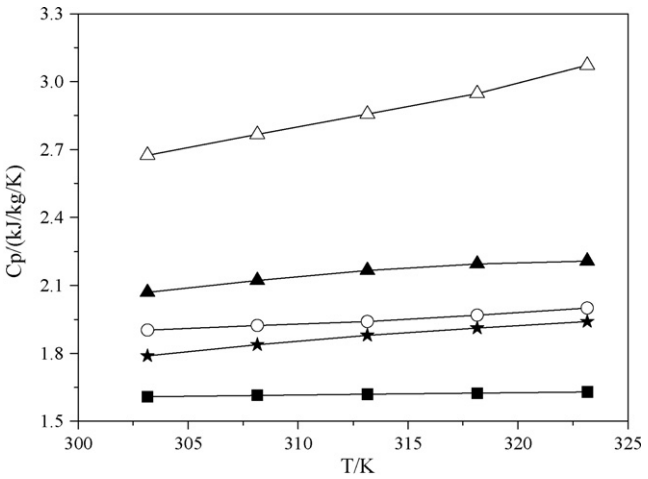

Fig. 4. The heat capacity of binary solution water (1) + EMISE (2) at different mole fractions of EMISE: Δ, 0.0987; ▲, 0.290; ◯, 0.499; ⋆, 0.691; ■, 1.

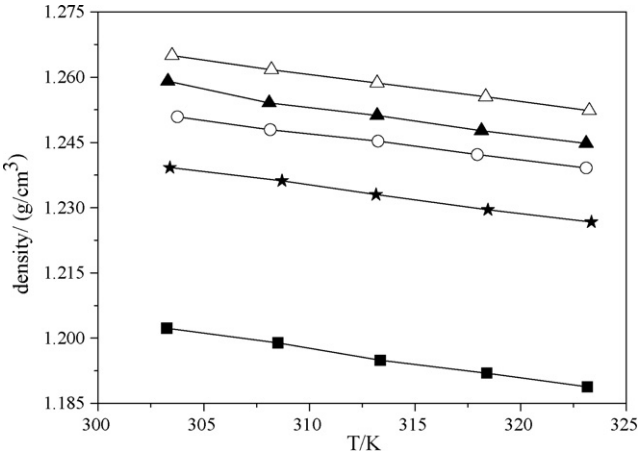

Fig. 5. The density of binary solution water (1) + EMISE (2) at different mole fractions of EMISE: Δ, 0.201; ▲, 0.480; ◯, 0.581; ⋆, 0.787; ■, 1.

Table 9
Parameters for the correlation of Eqs. (9) and (10).

	Heat capacity Eq. (9)	Density Eq. (10)
a_0	−4.7891	1.1390
b_0	2.6444×10^{-2}	-4.5170×10^{-4}
a_1	2.9481×10	2.3411
b_1	-1.1768×10^{-1}	-3.396×10^{-3}
a_2	-5.2435×10	−4.5764
b_2	2.0346×10^{-1}	8.0504×10^{-3}
a_3	2.9031×10	2.5755
b_3	1.1112×10^{-1}	-4.8930×10^{-3}

3.3. Density

Table 6 shows the density values of the binary system for temperature from 303.15 to 323.15 K and for molar fraction of the EMISE from 0 to 1. The density values decrease with increasing temperature and water mole concentration. All data were regressed by Eq. (10) [22].

$$\rho\,(\mathrm{g/cm^3}) = \sum_{i=0}^{3}(a_i + b_i T)x^i \qquad (10)$$

where ρ is the density the solution in g/cm, T is the absolute temperature in K, a_i and b_i are the regression parameters, and x is the molar fraction of the EMISE. The regression parameters were determined by the least-squares method and listed in Table 9 and plotted in Fig. 5. The average relative deviation (ARD) between the experimental and calculated values was 0.8%.

4. Conclusions

The novel ionic liquid absorbent, EMISE, for an absorption heat pump has been proposed.

The working pairs EMISE + H_2O has been considered as a potential working pair for the first time. The vapor pressure, heat capacity and density of the EMISE + H_2O system were measured, which are basic thermodynamic properties of the candidate working fluid used in an absorption heat pump. The vapor pressures were calculated using the NRTL model with the new parameters and showed good agreement with the experimental data. The temperature dependency parameters of the NRTL model were obtained by fitting the experimental VLE data. The experimental heat capacity and density were satisfactorily correlated with the simple polynomial functions of temperature and molar fraction. The average absolute deviations for the vapor pressure, heat capacity and density were 1.9%, 1.2%, and 0.8%, respectively.

Acknowledgement

The authors would like to thank the Chinese Natural Science Foundation Committee for supporting the project of the thermodynamic nature and cycle performance of new working pairs containing ionic liquid for high-temperature absorption heat transformer (no. 50876014).

References

[1] C.Z. Zhuo, C.H.M. Machielsen, Rev. Int. Froid. 16 (1993) 357–363.
[2] J.-W. Lee, K.-S. Kim, H. Lee, J. Chem. Eng. Data 48 (2000) 314–316.
[3] R.D. Rogers, K.R. Seddon, Ionic liquid solvents of the future, Science 302 (2003) 792–793.
[4] K.R. Seddon, Ionic liquids: a taste of the future, Nat. Mater. 2 (2003) 363–365.
[5] K.E. Herold, R. Radermacher, S.A. Klein, Absorption Chillers and Heat Pumps, CRC Press, 1996.
[6] W.F. Stoecker, J.W. Jones, Refrigeration and Air Conditioning, McGraw-Hill, 1982.
[7] F. Ziegler, Int. J. Therm. Sci. 38 (1999) 191–208.
[8] J.D. Holbrey, W.M. Reichert, R.P. Swatloski, G.A. Broker, W.R. Pitner, K.R. Seddon, R. Rogers, Green Chem. 4 (2002) 407–413.
[9] K. Michael, W. Peter, G. Jurgen, J. Chem. Eng. Data 47 (2002) 1411–1417.
[10] J.-W. Lee, K.-S. Kim, H. Lee, J. Chem. Eng. Data 48 (2003) 314–316.
[11] P. Bonhote, A.P. Dias, N. Papageorgiou, K. Kalyanasundaram, M. Gratzel, Inorg. Chem. 35 (1996) 1168.
[12] M.J. Earle, J.M.S.S. Esperance, M.A. Gilea, J.N.C. Lopes, L.P.N. Rebelo, J.W. Magee, K.R. Seddon, J.A. Widegren, Nature 439 (2006) 831–834.
[13] J.-F. Wang, C.-X. Li, Z.-H. Wang, Z.-J. Li, Y.-B. Jiang, Fluid Phase Equilibria 255 (2007) 186–192.
[14] J. Zhao, X.-C. Jiang, C.-X. Li, Z.-H. Wang, Phase Equilibria 247 (2006) 190–198.
[15] Y. Huo, S. Xia, S. Yi, P. Ma, Fluid Phase Equilibria 276 (2009) 46–52.
[16] Dalian University of Technology, Chemical Engineering Principle. Higher Education, 2002, p. 382.
[17] Z.-H. Zhang, Z.-C. Tan, L.-X. Suna, Y. JiaZhen, X.-C. Lv, Q. Shi, Thermochim. Acta 447 (2006) 141–146.
[18] W. Wagner, A. Pruss, The IAPWS formulation 1995 for the thermodynamic properties of ordinary water substance for general and scientific use, J. Phys. Chem. Ref. Data 31 (2002) 387–537.
[19] M.B. Shiflett, A. Yokozeki, AIChE J. 52 (2005) 1205–1219.
[20] M. Ishikawa, H. Kayanuma, N. Isshiki, Proc. Int. Sorption Heat Pump Conf., 1999, p. 197.
[21] J.-S. Kim, Y. Park, H. Lee, J. Chem. Eng. Data 42 (1997) 371–373.
[22] K.-S. Kim, H. Lee, J. Chem. Eng. Data 47 (2002) 216–218.